ELSEVIER

Earth and Planetary Science Letters 190 (2001) 237–250

EPSL

www.elsevier.com/locate/epsl

Weak zone formation for initiating subduction from thermo-mechanical feedback of low-temperature plasticity

J.M. Branlund [a], K. Regenauer-Lieb [b,*], D.A. Yuen [a]

[a] *Minnesota Supercomputer Institute and Department of Geology and Geophysics, University of Minnesota, Minneapolis, MN 55415-1227, USA*

[b] *Institute für Geophysik, ETH-Hönggerberg, Swiss Federal Institute of Technology, 8093 Zurich, Switzerland*

Received 13 December 2000; received in revised form 29 May 2001; accepted 31 May 2001

Abstract

We have addressed the problem of subduction initiation with a solid-mechanical and fluid-dynamical approach, using a finite-element method. The setup has been extended by a rate-sensitive coupling at the bottom of a semi-brittle lithosphere and a fully coupled thermo-mechanical model. The central element of our model is a broad asymmetric sedimentary loading function at the passive continental margin, which grows with time to 15 km. Two fundamentally different modes of shear zone formation have been found depending on the rheology of the creep layer. Mode 1: For cases of low or absent yield stress in the creep layer only, the semi-brittle top develops a weak zone, while the rate-sensitive layer acts as a decoupling shear zone. Mode 2: For cases with a yield strength in the creep layer (strain rates above 10^{-15} s^{-1} after yielding), the entire mechanical lithosphere fails on a major shear zone; mode 1 fails to model subduction initiation, while mode 2 creates a weak, major shear zone that severs through the entire lithosphere.

Keywords: subduction; rheology; thermo-mechanical properties; geodynamics; faults

1. Introduction

While the problem of subduction initiation at passive margins has been explored for a long time, it remains unresolved. McKenzie [1] was the first to point out that there must exist a state of delicate equilibrium, implying a very narrow parameter range and a unique rheological structure, for stable plate tectonics to exist like on Earth. He used a simple linear stability analysis and showed that a relatively high vertical displacement rate of at least 1 cm/yr is required at the ocean–continent boundary (OCB) to produce an instability on a preexisting weak zone. It remained totally unclear what mechanism could cause such a high vertical displacement rate before instability. Later on, analytical work investigated the problem with more refined lithospheric rheologies [2]. The authors came up with the solution that if the strength of the OCB fault were controlled by Byerlee's law, subduction initiation is impossible. Using the

* Corresponding author. Tel.: +41-1-633-2058; Fax: +41-1-633-1065.

E-mail address: klaus@tomo.ig.erdw.ethz.ch (K. Regenauer-Lieb).

0012-821X/01/$ – see front matter © 2001 Published by Elsevier Science B.V.
PII: S0012-821X(01)00393-4

weak fault assumption, Toth and Gurnis [3] reproduced subduction initiation with a 2-D finite-element model and viscoelastic rheologies. A slab forms at the site of the preexisting fault that cuts the lithosphere; the ridge push force required is on the same order as that predicted by McKenzie [1], for a weak fault strength below 10 MPa. Slab formation on preexisting weaknesses also occurred in analogue models [4,5]. An alternative kinematic convergence model for subduction initiation has been suggested based only on a viscous rheology [6].

The difficulty of initiating subduction with realistic rheology and geophysically relevant forces has led to different theories, on which strong forces play a significant role in subduction. Different scenarios, such as temporal changes in horizontal forces and anomalous heating of the ocean–continent margin, have been proposed [7]. Others have proposed that a tensile state of stress, not compression, promotes subduction initiation [8], supported by an analytical approach [9]. Some authors concluded that subduction does not initiate at passive margins, but rather in younger ocean basins [10] or as propagation (swarming) of existing subduction zones [2]. Cloetingh et al. [10,11] added a sedimentary load and ridge push force to a 2-D elasto-plastic finite-element model. Their model does not include a preexisting weakness (a lithosphere-cutting fault) at the OCB. Their steady-state results show that stresses in an old oceanic lithosphere with a depth-dependent yield stress envelope never reached the yield stress through an entire vertical slice of the OCB. They therefore concluded that subduction would not initiate on old passive margins.

Lithospheric strength estimates have recently shown [12] that the oceanic lithosphere is considerably weaker than previously thought (Fig. 1). The strength estimates have now reached a reasonable level of robustness, in spite of the notoriously large uncertainty ranges brought in by extrapolating laboratory data to natural conditions. This rheological model splits the traditional brittle layer into a brittle and a semi-brittle layer with a significantly lower strength than implied by the classical strength envelope [13]. We will investigate here the role of the semi-brittle layer in the formation of a weak zone for subduction initiation. Going one step further, we will observe the propagation of ductile shear bands into the creep layer. Particular emphasis is put on the thermo-mechanical role played by the Peierls mechanism in forming the weak zone [14].

In previous analyses, we have focused on the nucleation of ductile shear bands in a two-layer lithosphere, using the concept of a semi-brittle layer overlying a power-law creep layer [15–18]. Recently, we have used an even simpler analysis to the problem investigated here [19], i.e. by treating the lithosphere as a single elasto-plastic (semi-brittle) layer. A finite-element [20] model has been used to investigate the role of non-linear, elasto-plastic, strain-hardening rheology in deforming the passive continental margins. For simplicity, a linear sedimentary load function at continental margins is selected to be the sole ingredient for our analysis.

2. The strength of the lithosphere

According to the new rheological concept [12], the lithosphere can be subdivided into a three-layer solid where a thick, semi-brittle (ductile) layer is sandwiched between a deep, high-temperature, power-law creep and an upper crustal brittle fracture regime. Kohlstedt et al. [12] adopted a nomenclature from Rutter [21] in which the top layer was termed 'brittle', the middle was called 'ductile' (semi-brittle, high-pressure fracture) and the bottom layer (crystal) 'plastic' (viscous creep).

Following a nomenclature suggested earlier [22], we prefer to substitute the term 'plastic' by 'creep' in order to avoid confusion with the continuum mechanics definition of 'plastic'. In continuum mechanics, a state of plasticity describes a material behavior above a limiting yield stress. The brittle and ductile layers of the crust are plastic media, i.e. they have an elasto-plastic yield stress. On the other hand, the creep regime could be modelled with an entirely fluid-dynamical viscous approach, i.e. without a yield stress. The three-layer brittle–ductile–creep model hereafter is referred to as the BDC model. In our numerical model we will consider the ductile and the creep

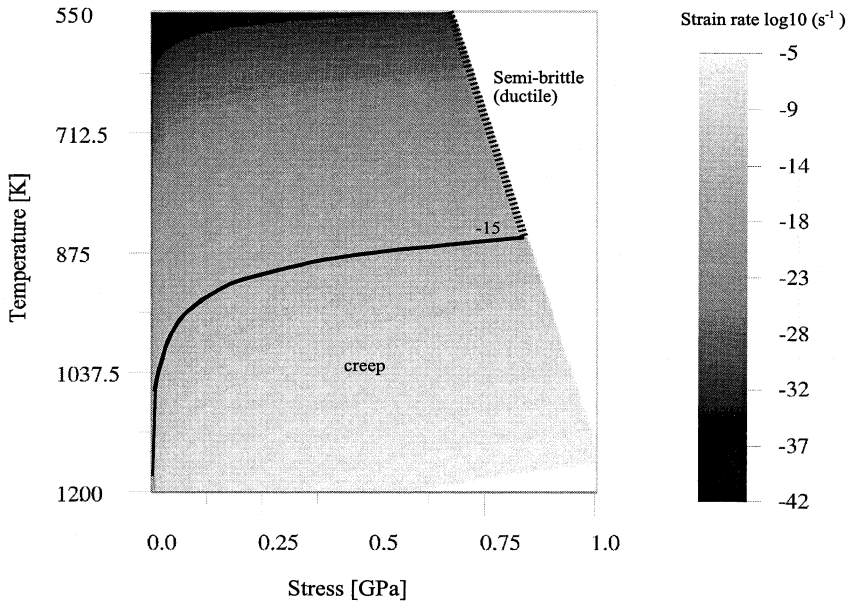

Fig. 1. Strength profile for the oceanic lithosphere according to a realistic rheological constraint [12]. The topmost brittle layer of negligible strength is not shown. The brittle strength is assumed to increase as a linear function of depth until at a depth greater than 10 km it is abandoned, in favor of the weaker semi-brittle (ductile) extrapolation shown here (dotted line). Kohlstedt et al. [12] use a reference strain rate of 10^{-15} s^{-1} to define the yield envelope. Instead of an envelope, we use a flow potential, which allows creep to take place above a yield limit defined in Fig. 2.

layers only. Reasons for neglecting the brittle layer are given below.

2.1. The brittle layer

In the strength envelopes constructed to illustrate the strength of the lithosphere, the yield strength of the upper crust is determined by the frictional strength of the material, since materials deform brittly at low temperatures and pressures. Byerlee's law [23] has been used to generalize the strength of pervasively faulted rocks within the top 10 km and beyond [24]. For the case of the oceanic lithosphere the brittle layer is most likely very thin and weak (in our case less than 10 km thick and less than one fifth of the ductile flow strength), so we neglect its effect in our first-order approximation of lithospheric rheology. In addition, sediments are included as a load (nodal force) only. Deformation within the sediment pile is undoubtedly occurring in a brittle manner, but is neglected.

2.2. The ductile layer and the upper yield stress

Fig. 1 only shows the ductile (semi-brittle) and creep layers of the BDC model. In the ductile layer, material no longer behaves entirely in a brittle manner, but deforms by a combination of dislocation glide and climb, as well as micro-brittle failure. The ductile–creep transition in turn marks the depth at which there is no longer any micro-brittle failure; below this depth all deformation is by dislocation climb or glide. These transitions bound the region of semi-brittle (ductile) flow.

The thickness of the ductile layer depends on the rate of deformation. The dashed line in Fig. 1 shows an example for a strain rate of 10^{-15} s^{-1}, which fails in a ductile manner below 875 K. For a higher strain rate, the ductile layer would be thicker. In the BDC model the uppermost stress limit allowed within the lithosphere is therefore defined by (semi-brittle)/ductile failure.

Experiments on the brittle–ductile transition are

scarce [25,26]. In lieu of more information, the ductile (semi-brittle) regime has been suggested to start [12] at the point were the brittle stress reaches one fifth of the creep stress. The ductile regime ends where the creep stress equals the effective confining pressure [13]. This criterion, also known as the 'Goetze criterion', introduces rate sensitivity for the depth of the ductile–creep transition, hence it also defines an upper yield stress for the creep regime. To represent the yield stress of the ductile region, a linear extrapolation between the strength obtained at the brittle–ductile transition and that obtained for the ductile–creep transition has been used [12].

In terms of fracture mechanics, the ductile layer shows strain localization (shear bands) that propagate under mode 2 conditions (shear bands) instead of the mode 1 (cleavage fracture). The initiation of shear bands can be modelled by a simple von Mises elasto-plastic formulation [15]. Here, we end the calculation after the shear band has been established, and do not go into the more evolved ductile fracture modes [17,27]. Von Mises elasto-plastic body yielding occurs when the stress reaches a finite yield stress τ_y, defined by the yield potential

$$\frac{J_2^2}{\tau_y^2} - 1 = 0 \tag{1}$$

where J_2 is the second invariant of the deviatoric stress tensor. Below this yield stress we ascribe the material as being entirely elastic, and when reaching this stress we use the additive strain rate decomposition:

$$\dot{\varepsilon}_{ij} = \dot{\varepsilon}_{ij}^{\mathrm{el}} + \dot{\varepsilon}_{ij}^{\mathrm{pl}} \tag{2a}$$

where the superscripts refer to elastic and plastic, respectively. Pressure and temperature effects are presumably present within the ductile layer [26], but given the experimental uncertainties, they are ignored here.

2.3. The creep layer

In the classical formulation of the strength of the lithosphere [13], the yield strength was defined by a constant strain rate (e.g. 10^{-15} s^{-1}) and other strain rates were not considered. In Fig. 1, we replace the yield envelope with a flow potential in order to fully implement the rate sensitivity. The rate of deformation in the creeping portion of the lithosphere consists of three contributions:

$$\dot{\varepsilon}_{ij} = \dot{\varepsilon}_{ij}^{\mathrm{el}} + \dot{\varepsilon}_{ij}^{\mathrm{L}} + \dot{\varepsilon}_{ij}^{\mathrm{P}} \tag{2b}$$

where the superscripts L and P refer to the low-temperature plastic and the power-law creep, respectively.

2.3.1. Low-temperature plasticity, the yield phenomenon in the creep regime

Low-temperature plasticity is a dislocation glide-controlled creep which occurs at high stresses and low temperatures [22]. The so-called 'Peierls stress' τ_{o}, is an ideal yield stress defined at low temperatures. The mechanism introduces ductility. The constitutive law for low-temperature plasticity is:

$$\dot{\varepsilon}_{ij}^{\mathrm{L}} = \dot{\varepsilon}_0 \exp\left(\frac{-Q_{\mathrm{L}}}{RT}\left(1-\frac{\tau_{ij}}{\tau_{\mathrm{o}}}\right)^2\right) \tag{3}$$

where $\dot{\varepsilon}_0$ is a reference strain rate in s^{-1}, τ_{o} is the Peierls stress, Q_{L} is the low-temperature plastic activation energy, R is the universal gas constant, and T the temperature in K and τ_{ij} is the Kirchhoff stress defined as:

$$\tau_{ij} = \frac{\mathrm{d}V}{\mathrm{d}V_0}\sigma_{ij} \tag{4}$$

$\mathrm{d}V/\mathrm{d}V_0$ is the Jacobian of elastic deformation between the original elastic volume and the current (at time t) volume; σ_{ij} is the complete Cauchy stress tensor [28].

2.3.2. Power-law creep

At higher temperatures and higher stresses, power-law creep (also called dislocation creep) dominates. Again, the pressure sensitivity does not play an important role in the oceanic lithosphere before subduction, and the constitutive law for power-law creep can be written as:

$$\dot{\varepsilon}_{ij}^{\mathrm{pl}} = A J_2^{n-1} \tau_{ij} \mathrm{e}^{-\frac{Q_{\mathrm{P}}}{RT}} \tag{5}$$

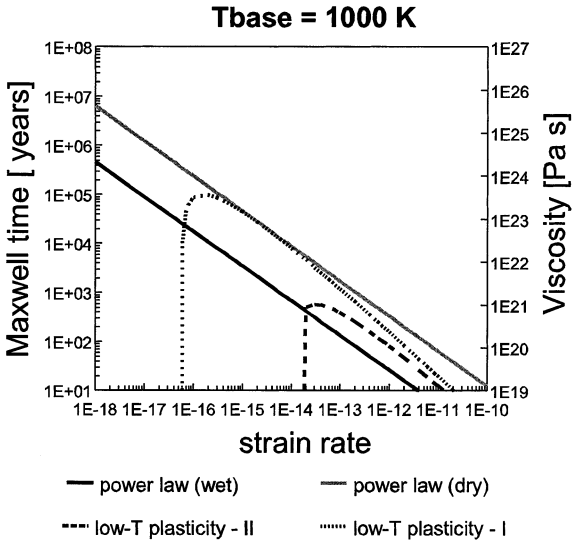

Fig. 2. The lower yield stress is obtained from the intersection of the low-temperature (T) plastic with the (power law) dislocation creep curves. Low-T plastic I refers to data from Goetze and Evans [13] and low-T plastic II to data published by Evans and Goetze [29]. Maxwell time indicates that a lithosphere with $T_{base} = 1000$ K can essentially be treated as an elastic body before yielding at its bottom for time-scales larger than 10 kyr. Alternatively, this plot can be interpreted as an effective viscosity map. The non-linearity of the low-T plastic yield phenomenon becomes apparent.

where A is a material constant, Q_P is the activation energy of the power-law rheology.

2.3.3. The lower yield stress in the creep regime

Three criteria define the creep model: (I) an upper yield stress, above which the material is perfectly plastic (Goetze criterion), (II) a lower yield stress defined as the stress above which dislocation glide can occur, and below which material is elastic, and (III) an area between the two yield stresses where it deforms by a composite power-law and low-temperature plastic creep.

While the upper yield stress is the von Mises yield stress (Eq. 1) defined above, the lower yield stress (Fig. 2) is defined on the basis of low-temperature plasticity and a particular isotherm, T_{base}. Next, the time frame of the deformation process must be specified for this particular isotherm. Low-temperature plasticity rate law and power law are used to calculate the Maxwell relaxation time ($t_M = \tau/(\dot{\varepsilon}\mu)$; where τ is the shear stress from the creep law, μ is the elastic shear modulus), or the time-scale over which a material exhibits considerable elastic strength. The low-temperature plasticity formulation, Eq. 3, gives an effective Maxwell time:

$$t_M = \frac{1}{\mu}\frac{\tau_0}{\dot{\varepsilon}}\left[1-\left(\frac{RT_{base}}{Q_L}\ln\left(\frac{\dot{\varepsilon}_0}{\dot{\varepsilon}}\right)\right)^{0.5}\right] \quad (6)$$

Inflections in the plot of effective Maxwell time can be observed at a strain rate where the material stops behaving elastically and creep starts with a characteristic strain rate. The stress that gives the strain rate is the lower yield stress, and can be calculated from the low-temperature plasticity-flow law. The inflections in the (t_M) plot occur at:

$$\frac{RT_{base}}{Q_L} ln\left(\frac{\dot{\varepsilon}_0}{\dot{\varepsilon}_{crit}}\right) = 1 \quad (7)$$

which is when:

$$\dot{\varepsilon}_{crit} = \dot{\varepsilon}_0 \exp\left(-\frac{Q_L}{RT_{base}}\right) \quad (8)$$

This defines the critical strain rate for the onset of low-temperature plastic creep at T_{base}, giving the lowermost yield stress in the lithosphere if T_{base} corresponds to the bottom of the mechanical lithosphere. However, at stresses lower than the upper yield stress, low-temperature plasticity is not the dominant deformation mechanism. Deformation occurs by power-law creep according to the rate law in Eq. 5, with data recommended by Kohlstedt et al. [12], at stresses between the lower and upper yield stress. Therefore, while the low-temperature plasticity-flow law is used to calculate the initial strain rate, the power-law creep-flow law (Eq. 5), inverted for the stress, is used to calculate the lower yield stress at this strain rate. We emphasize here that the use of a yield potential based on the experimentally better explored power law is only valid for oceanic lithosphere prior to subduction. Once the lithosphere is deeply subducted, the Goetze criterion can no longer be used to extrapolate the upper yield stress. At such high stress, low-temperature plasticity must be explicitly implemented via Eq. 2b,

which then defines the upper, as well as the lower, yield stress.

3. The thermal, mechanical and elastic thickness of the lithosphere

From this approach, the lithospheric strength is defined based alone on the shape of the continental margin and the associated thermal model. We do not consider additional complexities, such as compositional variation between the oceanic and continental lithosphere. It is assumed here that the uncertainty in the thermal model can be expressed in terms of the differences between the cooling half space and cooling plate models of the oceanic lithosphere [30]. Using this approach, the base of the thermal lithosphere hence can be defined following an isotherm, e.g. the 1600 K isotherm [31].

Several measurements of the elastic thickness of oceanic lithosphere have been made (see [32] for a review). They show that elastic thickness increases with thermal age, typically following an isotherm of about 720 K.

Ranalli [33] derived a non-linear flexural rigidity parameter using a strain-hardening plasticity model (discussed later) similar to the Ramberg–Osgood model in our single-ductile-layer analysis [19]. The base of the mechanical lithosphere (oceanic), like the thermal and elastic lithospheres, can also be defined by an isotherm. The isotherms proposed for the base of the mechanical lithosphere vary from $T_{\mathrm{base}} = 973$ K to 1173 K [33,34].

Given this range of values for T_{base}, and the fact that Q_{L} and $\dot{\varepsilon}_0$ in Eq. 8 are only known from two micro-indentation experiments [13,29], we have kept $\dot{\varepsilon}_{\mathrm{crit}}$ as a free parameter within reasonable bounds (10^{-11} and 10^{-20} s^{-1}). The power-law creep rate law (Eq. 5), with $T = 1173$ K, is used to calculate the lower yield stress, i.e. the stress at the reference strain rate. Between the upper and lower yield stress, material deforms by power-law creep, again following Eq. 5. The reference strain rate is the minimum strain rate used to determine the model rheology.

The temperature dependence of both the lower yield stress and power-law creep creates (a) a depth-dependent strength and (b) a shear-heating feedback in the model. Initial temperatures are determined from a linear geotherm with a 573 K Moho temperature and a 1173 K isotherm at the base of the model. The time-dependent energy equation in Lagrangian form is [15]:

$$\frac{\mathrm{D}T}{\mathrm{D}t} = \kappa \nabla^2 T + \frac{\psi}{\rho C_{\mathrm{p}}} \tau_{ij} \dot{\varepsilon}_{ij}^{\mathrm{pl}} \tag{9}$$

where the term D/Dt refers to substantive derivative, ψ is the efficiency of converting anelastic work to shear heating, and κ is the diffusivity. The second term therefore expresses the shear-heating term. In the creep layer, $\dot{\varepsilon}_{ij}{}^{\mathrm{pl}}$ is replaced by the equivalent $\dot{\varepsilon}_{ij}{}^{\mathrm{P}}$. The method for advection of stress, deformation of the top free surface and the time stepping procedure for our fully coupled temperature-displacement analysis, is the same as described earlier [16–18]. We are using the finite-element code ABAQUS [20].

4. Model geometry, boundary conditions

The model consists of an oceanic lithosphere that thickens closer to the continental margin and a small section of the continent, where the OCB marks the break in slope between the oceanic and continental lithospheres (Fig. 3). The geometry is meshed into 9900 rectangular elements, with the highest resolution at the OCB [19] where the elements are square. The dimensions of the elements closest to the OCB are 900×900 m. The mesh coarsens towards the boundaries, which are placed far enough away from the area of interest (the OCB) to avoid any boundary effects.

Because the continental lithosphere is expected to be thinned at the rifted margin, it is given a thickness (40 km) just slightly larger than the oceanic thickness (27 km at the OCB).

The choice of our initial lithosphere thickness distribution is governed by the saturation of strength implied by a cooling plate model, as opposed to a linear increasing sediment load. The key question is whether the given incremental sediment load can become sufficiently high to

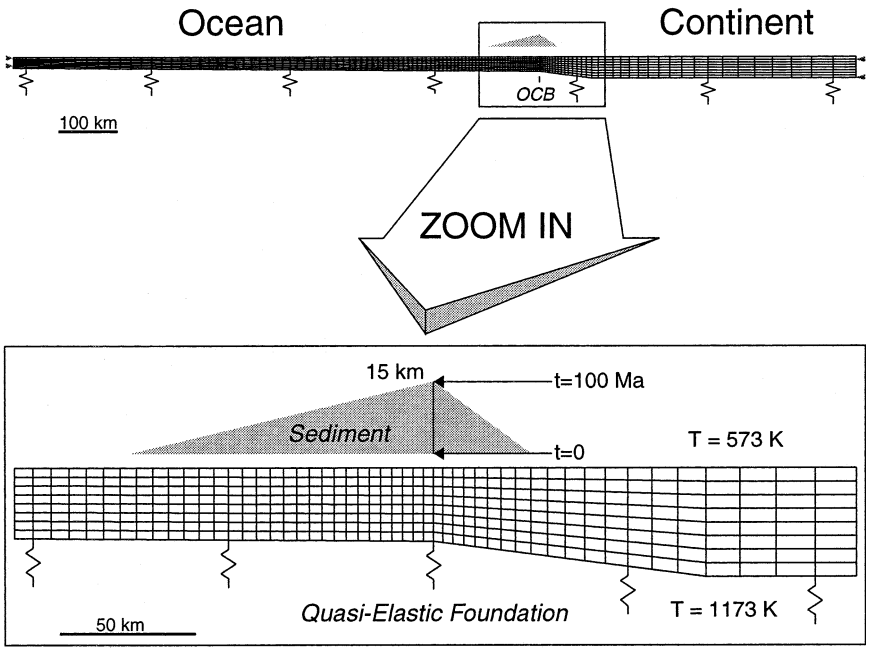

Fig. 3. Simple model setup of the OCB with sediment loading. Sediment loading is the sole ingredient [10]. In this work we investigate the question whether sediment loading alone can act as a precursor to subduction initiation by making use of the new rheological concept of the oceanic lithosphere [12].

cause whole-scale failure. In the extreme case of a very high sedimentation rate, ductile failure is implied for a young oceanic lithosphere [10]. However, for reasonable sedimentation rates, the same authors conclude that the lithosphere cannot break, but that the lithosphere will preserve an elastic high strength central segment. We use the BDC model to investigate subduction initiation for a mature oceanic lithosphere of an age larger than 50 Myr. We consider an upper bound of thermal parameters as implied by the cooling half space model at a maximum thermal age of 100 Myr.

Within the plausible range of parameters set at the outset, our numerical model has the advantage of predicting self-consistently where the bottom of mechanical lithosphere can be expected.

4.1. The sediment load and isostatic restoring forces

A triangular sediment load with ρ^s of 2400 kg/m^3 is added to the top of the lithosphere with its maximum height at the OCB. The load thins to zero at either side of the OCB giving a maximum load width of 150 km. Approximately 70% of the load is oceanward of the OCB. The height of the sediment wedge grows linearly with time from 0 to 15 km in 100 Ma. The sediment load is applied as a nodal force, and has no internal strength.

Displacement from the sediment load is counteracted to some degree by an isostatic restoring force [35], representing the positive buoyancy of the displaced asthenosphere. The restoring force is implemented by adding a spring element to the base of each column of nodes. The springs can only act when there is a vertical displacement of the basal node.

5. Results

The elasto-plastic model without rate sensitivity [19] is reproduced here in Fig. 4 for the purpose of comparison. This model gives a shear zone that

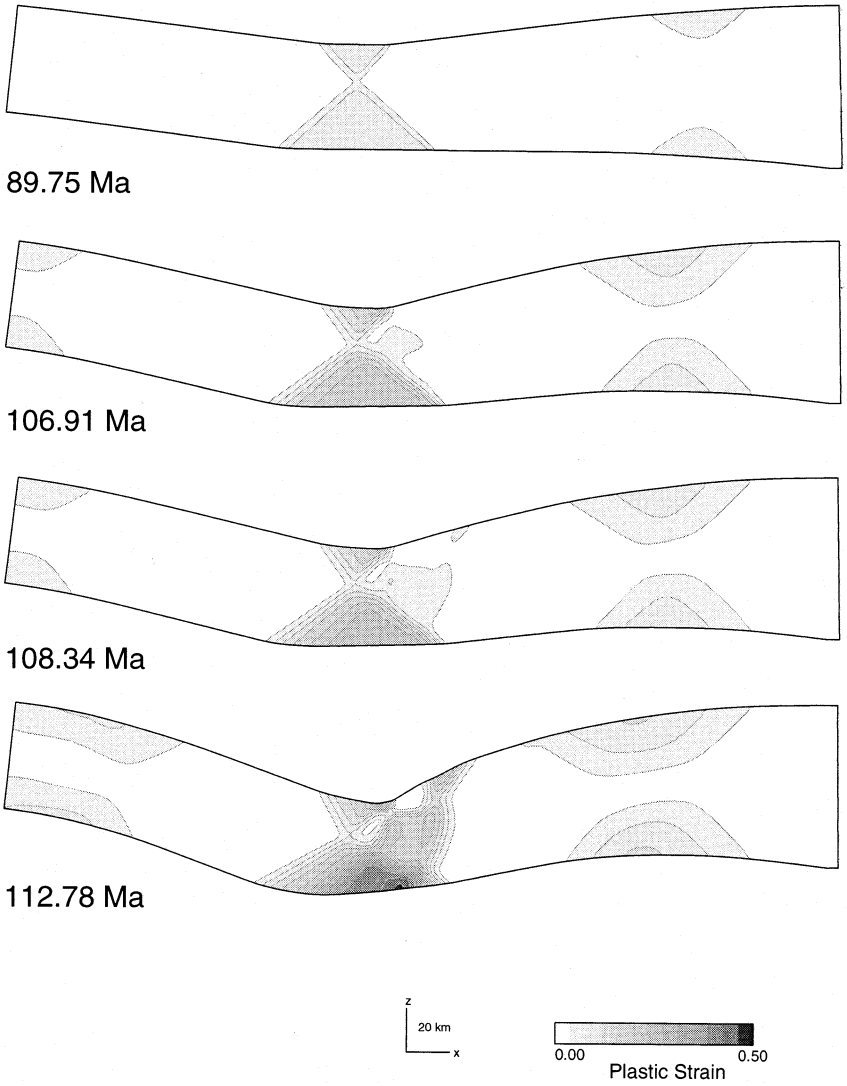

Fig. 4. Mode 0 deformation for the single elasto-plastic plate with a yield stress of 200 MPa [19]. Shear bands on the OCB form as a result of sediment loading. Mode 0 requires the full sediment load of 15 km to cause formation of a weak zone. The equivalent plastic strain contours are defined by integrating the increments of plastic strain ($\int \sqrt{(2/3)\mathrm{d}\varepsilon_{ij}\mathrm{d}\varepsilon_{ij}}$).

grows from the base of the lithosphere to the Moho, with an oceanward dip (mode 0). In the elasto-plastic model stress is expected to increase with the strain, owing to an increase of the dislocation density during deformation. This effect is particularly prominent for metals. Addition of such strain hardening causes the plastic strain to be less localized. The diffuse shear zones, in cases with high amounts of strain hardening, forms over much longer time-scales than the perfectly plastic shear zones. Using strain-hardening data for olivine, we found that the effect is negligible [19]. With a relatively low yield stress of 200 MPa, a shear zone will form through the entire model lithosphere, but a full sediment load of 15 km is required.

The addition of the viscous component induces a wide range of deformation styles with two end-

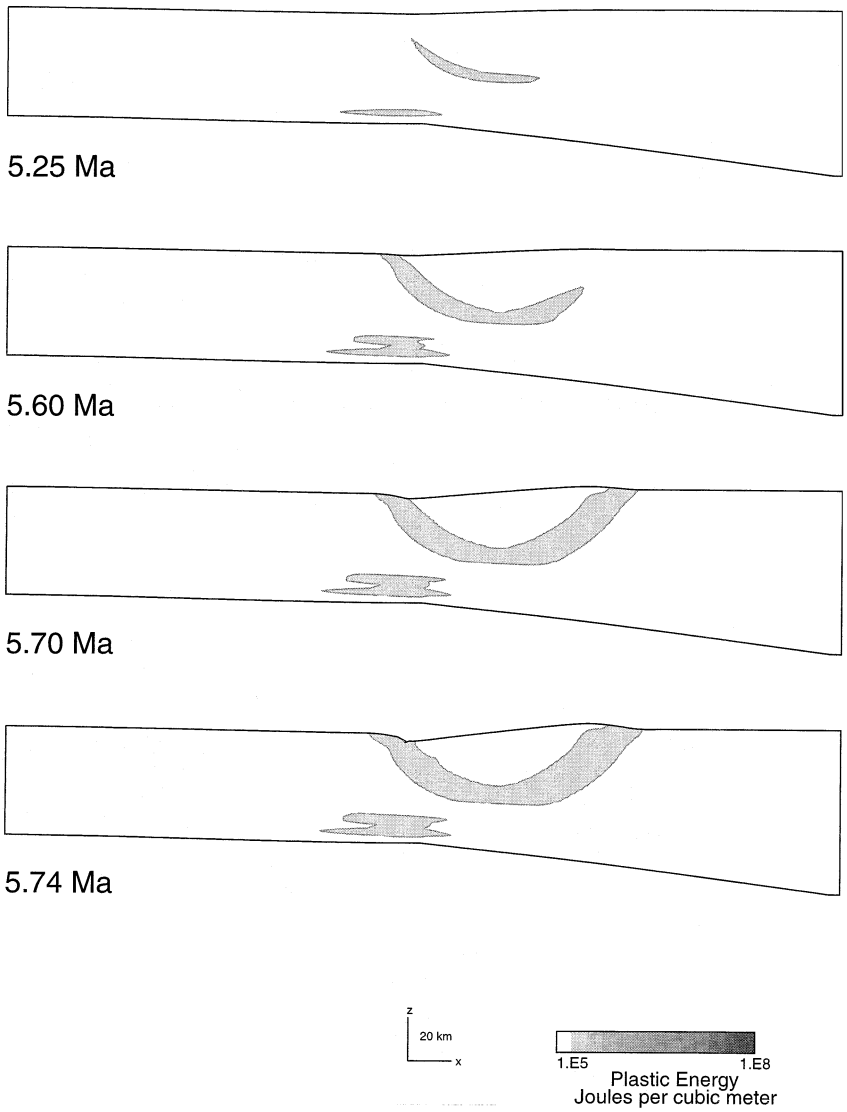

Fig. 5. Mode 1 deformation for a two-layer ductile–creep model with low or absent yield stress in the creep layer. Contour lines show the plastic and viscous energy dissipated on the shear zone. This energy is converted into heat (Eq. 9). A sediment load of only 2 km is required to break a very thin lithosphere.

members. In the first end-member (mode 1, Fig. 5), the lithosphere appears to be too weak and thin. A sediment load of only 1 km is required to cause viscoelastic deformation in the middle of the plate beneath the load. A shear zone that dips towards the continent forms, and soon after a shear zone that dips toward the ocean forms. The two shear zones form a 'U', and the base of the 'U' marks a characteristic depth that corresponds to the base of a very thin mechanical lithosphere. Plastic deformation does not extend through the entire model lithosphere. In addition, continued loading (not shown) causes only the rotation of the block within the 'U', and subsidence is limited by a characteristic depth. The rotation is a good illustration where considering the importance of taking the Jaumann stress terms into account is imperative [17].

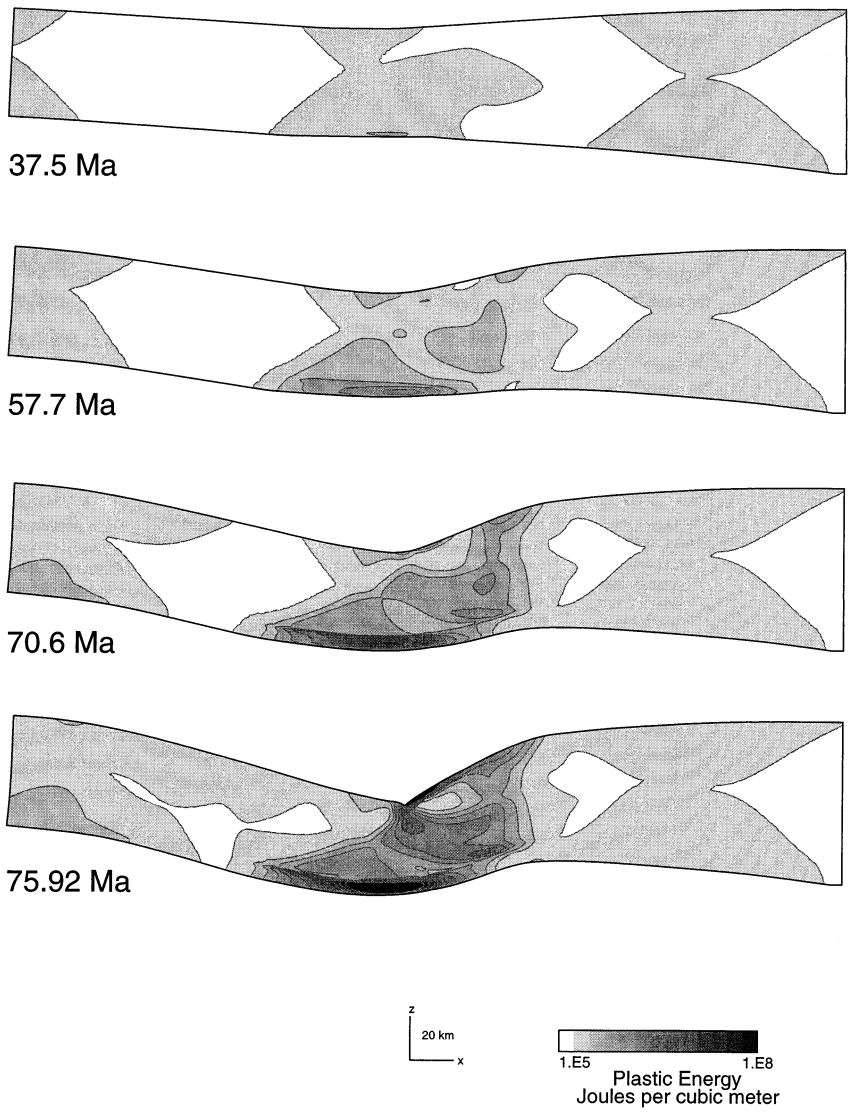

Fig. 6. Mode 2 deformation for a two-layer ductile–creep model including a low yield stress in the creep layer (critical strain rate of 10^{-15} s^{-1}). The lithosphere breaks under a sediment load of 10 km. This model can explain the formation of a weak zone for subduction initiation.

The mode 2 (Fig. 6) end-member resembles the perfectly plastic solution, with the plastic strain occurring throughout the entire model lithosphere thickness. Rate-sensitive coupling at the bottom of the lithosphere adds some complexity to the shear zones however. The amount of plastic and viscous energy dissipation is much higher in mode 2 cases than in mode 1 cases, being significant not only at the OCB, but in the two hinge zones as well. Viscous energy dissipation is highest at the base of the model lithosphere beneath the load. In our model runs, viscous energy dissipation is not high enough to cause significant heating of the lithosphere. Energy does focus in a continent-dipping-curved shear zone that bears some resemblance to the 'U'-shaped mode 1 shear zone. In

mode 2, the base of the mechanical lithosphere coincides with the validity domain of the effective Peierls stress mechanism. In mode 1, the base of the mechanical lithosphere is defined by the ductile–creep transition, giving the characteristic depth of decoupling deformation. The characteristic depth of the ductile–creep transition is a function of the activation energy, reference strain rate and temperature.

6. Implications for initiating subduction

The results for perfect plasticity (mode 0) suggest that a reasonable sediment load placed on an ocean–continent margin can cause the lithosphere to break. The break may be the first stage in subduction initiation by producing a weak zone that enables negative buoyancy forces to become large enough to start pulling the oceanic lithosphere into the mantle, creating a slab-like structure. This simple solution is appealing, but uses 200 MPa yield stress, which probably underestimates the true yield stress of the lithosphere and requires a thick sediment pile for failure (15 km). While there are some localized areas with high sedimentation rates, few basins have a sediment thickness greater than 15 km. It is therefore hard to justify adding a larger sediment pile. This study shows that inclusion of a lower yield stress and a viscous component will allow for failure with far less than a 15 km sediment load through visco-elastic stress amplification at the bottom of the lithosphere. Whether a sufficiently large portion of the lithosphere can break (mode 2, reference strain rate set to 1×10^{-15} s^{-1}) or not (mode 1, reference strain rate set to 1×10^{-16} s^{-1}) depends on the reference strain rate and the rheological parameters of the material (higher strain rates and higher activation energies favor whole-scale lithospheric failure Fig. 6).

The mechanical thickness estimates based on measurements of elastic thickness suggest that the base of the mechanical lithosphere follows an isotherm between 973 and 1173 K [33,34]. If experimentally derived activation energies are valid, the reference strain rate of the lithosphere must be greater than 1×10^{-16} s^{-1} for the base of the mechanical lithosphere to follow a 973 K isotherm in mode 2 deformation. A reference strain rate of 1×10^{-15} s^{-1} is needed for the 1173 K isotherm.

The addition of a viscous component to an elasto-plastic lithosphere promotes lithospheric failure. Failure according to mode 1 deformation can occur at slower strain rates in materials with higher values of activation energy (greater than 550 kJ/mol). However, such high activation energies are not supported on the basis of laboratory data [12]. Therefore, we prefer a flow potential for the lithosphere that has two finite yield limits. We define a lower yield stress at the bottom of the mechanical lithosphere by Eqs. 5 and 8, and an upper yield stress in the semi-brittle regime by the Goetze criterion.

7. Discussion

The fact that a thick sediment pile of O (10 km) placed at the OCB is sufficient to cause ductile failure of the lithosphere should be of no surprise. This implies a lower strength of the oceanic lithosphere than previously thought. There are some subtleties to this, which must not be overlooked. In a purely elasto-plastic setup (mode 0, Fig. 4) the lithosphere appears rather strong and only breaks under excessive sediment loading (15 km thick). Visco-elastic deformation in the rate-sensitive layer at the bottom of the lithosphere is an important helper because it precedes failure of the ductile regime and helps in building up stresses for failure. This visco-elastic stress amplification [36] is so strong that the ductile layer can and will fail under 2 km sediment loading only (mode 1, Fig. 5) if the lower yield stress phenomenon is neglected or insignificant. The lower yield stress has the effect of synchronizing deformation in the ductile and creep layers, as well as storing elastic energy to be released upon whole-scale lithospheric failure. When this occurs, the maximum energy dissipation is in the immediate vicinity of the bottom of the ductile layer (Fig. 6). Owing to the exponential dependence of viscosity on temperature, thermo-mechanical feedback instabilities are likely to occur in the rate-sensitive domain [14].

Significant shear heating has not been observed under the relatively low sedimentation rates used in this study. The system is, however, collapsing rapidly, so that by consideration of ridge push forces or higher loading rates, thermally triggered seismic instabilities [16,17] may be possible.

The question of the influence of the shape and width of the sedimentary loading function needs to be discussed briefly. An interesting aspect would be introduced by including a sediment load-dynamic-geometry feedback mechanism. It turns out that the philosophy of the approach must change slightly. In a geometry feedback analysis we can no longer take a simplified load of the present image of Atlantic-type continental margin sedimentation (since it is a function of the plastic collapse), but have to consider an initial (broader wavelength) sedimentation model, which then should develop dynamically into a reproduction of an Atlantic-type continental margin. We have run experiments with a different range of the initial sedimentary loading functions before releasing a dynamic geometry-sedimentation feedback, and found that a refined approach gives a richer solution space. There appears a new subgroup to the fundamental mode 2. In addition to the initial wavelength, a second short 'collapse' wavelength appears, which is missing in the simple model shown here. A narrower load in mode 2 also implies that the lithosphere breaks more rapidly and more refined on a narrow 'hinge line'. This feedback mechanism will not affect our key message of the existence of two fundamental modes of deformation.

Our analysis shows that a full thermo-rheological setup is needed for modeling the oceanic lithosphere with realistic Earth material parameters. If, for instance, non-linear yielding is neglected and the lithosphere is treated as a linear visco-elastic solid, the activation energy must be selected to be as low as the order of 100 kJ/mol [37] to mimic non-linear (ductile) lithosphere failure in a smoothed-out fashion. This value is lower than even a wet rheology in the diffusion creep regime may suggest and it shows that the lithosphere must be made artificially malleable. This behavior is in stark contrast to the apparent rigidity of the oceanic lithosphere. The dichotomy, strong before failure and soft upon failure, is fully incorporated in the non-linear modelling process.

8. Conclusions

The results of this work offer the first possibility of a straightforward definition for the mechanical nature of the lithosphere in the P and T domain of low-temperature plasticity, the Peierls mechanism. The validity domain depends on the time frame of deformation and the critical stress state in the lithosphere. If a critical state can be reached within a time frame of 100 kyr, a ductile shear band can propagate into the 1000 K isotherm (Fig. 6). We have shown that such thermo-mechanical critical states can be reached even in the case of a slow sediment loading rate.

This work has also important ramifications for modeling the lithosphere by fluid-dynamical approaches. In such approaches, one should add a Bingham plastic model [38], representing the lower yield stress, to the standard pseudo-plastic [39] model, representing the high yield stress. This has the advantage of a simple objective model definition of the mechanical lithosphere by the validity range of the Peierls mechanism below about 1225 K [29].

We have shown in this paper that the thermodynamics of low-temperature plasticity has a fundamental impact on initiating localized deformation within the lithosphere. It is the first and foremost mechanism for propagating ductile shear bands into the creep regime. Secondary instabilities, such as void-volatile feedback [27,40], thermally triggered seismic instabilities [16] and grain-size-sensitive feedback [41,42], all rely on preparatory thermo-mechanical weakening by low-temperature plasticity.

Acknowledgements

We would like to thank Louis Moresi, Marc Parmentier and Chad Hall for a very helpful review. This work has been jointly funded by the ETH Zurich and the University of Minnesota in a

project that should have become a PhD. degree of the first author. We regret that Joy preferred to finish with a Master's degree. This is publication 1184 of the Institute of Geophysics ETH Zurich. *[RV]*

References

[1] D.P. McKenzie, The initiation of trenches: a finite amplitude instability, in: M. Talwani, W.C. Pitman (Eds.), Island Arcs Deep Sea Trenches and Back-Arc Basins, Vol. 1, Maurice Ewing Ser., 1977, pp. 57–61.

[2] S. Mueller, R. Phillips, On the initiation of subduction, J. Geophys. Res. 96 (1991) 651–665.

[3] G. Toth, M. Gurnis, Dynamics of subduction initiation at preexisting fault zones, J. Geophys. Res. 103 (1998) 18053–18067.

[4] A.I. Shemenda, Horizontal lithosphere compression and subduction: constraints provided by physical modeling, J. Geophys. Res. 97 (1992) 11097–11116.

[5] A.I. Shemenda, Subduction of the lithosphere and back arc dynamics: insights from physical modeling, J. Geophys. Res. 98 (1993) 16167–16185.

[6] C. Faccenna et al., Initiation of subduction at Atlantic-type margins: Insights from laboratory experiments, J. Geophys. Res. 104 (1999) 2749–2766.

[7] S.G. Ericksson, J. Arkani-Hamed, Subduction initiation at passive margins: The Scotian Basin, Eastern Canada as a potential example, Tectonics 12 (1993) 678–687.

[8] D.V. Kemp, D.J. Stevenson, A tensile, flexural model for the initiation of subduction, Geophys. J. Inl. 125 (1996) 73–94.

[9] G. Schubert, K. Zhang, Foundering of the lithosphere at the onset of subduction, Geophys. Res. Lett. 24 (1997) 1527–1529.

[10] S.A.P.L. Cloetingh, M.J.R. Wortel, N.J. Vlaar, Evolution of passive continental margins and initiation of subduction zones, Nature 297 (1982) 139–142.

[11] S. Cloetingh, R. Wortel, N.J. Vlaar, On the initiation of subduction zones, Pure Appl. Geophys. 129 (1989) 7–25.

[12] D.L. Kohlstedt, B. Evans, S.J. Mackwell, Strength of the lithosphere: Constraints imposed by laboratory measurements, J. Geophys. Res. 100 (1995) 17587–17602.

[13] C. Goetze, B. Evans, Stress and temperature in the bending lithosphere as constrained by experimental rock mechanics, Geophys. J. R. Astron. Soc. 59 (1979) 463–478.

[14] C. Kameyama, D.A. Yuen, S. Karato, Thermal-mechanical effects of low temperature plasticity (the Peierls mechanism) on the deformation of a viscoelastic shear zone, Earth Planet. Sci. Lett. 168 (1999) 159–162.

[15] K. Regenauer-Lieb, D. Yuen, Rapid conversion of elastic energy into shear heating during incipient necking of the lithosphere, Geophys. Res. Lett. 25 (1998) 2737–2740.

[16] K. Regenauer-Lieb, D. Yuen, Quasi-adiabatic instabilities associated with necking processes of an elasto-viscoplastic lithosphere, Phys. Earth Planet. Inter. 118 (2000) 89–102.

[17] K. Regenauer-Lieb, D.A. Yuen, Fast mechanisms for the formation of new plate boundaries, Tectonophysics 322 (2000) 53–67.

[18] K. Regenauer-Lieb, J.P. Petit, D. Yuen, Adiabatic shear bands in the lithosphere: Numerical and experimental approaches, Electron. Geosci. 4 (1999) 2.

[19] J. Branlund, K. Regenauer-Lieb, D. Yuen, Fast ductile failure of passive margins from sediment loading, Geophys. Res. Lett. 27 (2000) 1989–1993.

[20] ABAQUS/Standard. User's Manual Vol. 1, Version 5.8, Hibbit, Karlsson and Sorenson Inc., 1999.

[21] E.H. Rutter, On the nomenclature of mode of failure transitions in rocks, Tectonophysics 122 (1986) 381–387.

[22] M.F. Ashby, R.A. Verall, Micromechanisms of flow and fracture, and their relevance to the rheology of the upper mantle, Philos. Trans. R. Soc. London 288 (1978) 59–95.

[23] J.D. Byerlee, Friction of Rocks, Pure Appl. Geophys. 116 (1978) 615–626.

[24] R.A. Albert et al., A test of the validity of yield strength envelopes with an elastoviscoplastic finite element model, Geophys. J. Int. 140 (2000) 399–409.

[25] G. Hirth, J. Tullis, The brittle–plastic transition in experimentally deformed quartz aggregates, J. Geophys. Res. 99 (1994) 11731–11747.

[26] M. Shimada, Lithosphere strength inferred from fracture strength of rocks at high confining pressures and temperatures, Tectonophysics 217 (1993) 55–64.

[27] K. Regenauer-Lieb, Dilatant plasticity applied to Alpine Collision: ductile void growth in the intraplate area beneath the Eifel Volcanic Field, J. Geodyn. 27 (1999) 1–21.

[28] Drozdov, A.D., Finite Elasticity and Viscoelasticity, World Scientific, Singapore, 1996, 300 pp.

[29] B. Evans, C. Goetze, The temperature variation of the hardness of olivine and its implications for the polycrystalline yield stress, J. Geophys. Res. 84 (1979) 5505–5524.

[30] R.L. Carlson, H.P. Johnson, Coooling half space and cooling plate models of the oceanic lithosphere, J. Geophys. Res. 99 (1994) 3201–3214.

[31] B. Parsons, J.G. Sclatter, An analysis of the variation of ocean floor bathymetry and heat flow with age, J. Geophys. Res. 83 (1977) 803–827.

[32] P. Wessel, Thermal stresses and the bimodal distribution of elastic thickness estimates of the oceanic lithosphere, J. Geophys. Res. 97 (1992) 14177–14193.

[33] G. Ranalli, Nonlinear flexure and equivalent mechanical thickness of the lithosphere, Tectonophysics 240 (1994) 107–114.

[34] E.B. Burov, M. Diament, The effective elastic thickness (Te) of continental lithosphere: What does it really mean?, J. Geophys. Res. 100 (1995) 3905–3927.

[35] D.L. Turcotte, J.H. Ahern, J.M. Bird, The state of stress at passive continental margins, Tectonophysics 42 (1977) 1–28.

[36] N.J. Kusznir, The distribution of stress with depth in the

lithosphere: thermo-rheological and geodynamic constraints, Philos. Trans. R. Soc. London Ser. A-Math. Phys. Eng. Sci. 337 (1991) 95–110.
[37] A.B. Watts, S. Zhong, Observation of flexure and the rheology of oceanic lithosphere, Geophys. J. Int. 142 (2000) 855–875.
[38] R. Trompert, U. Hansen, Mantle convection simulations with rheologies that generate plate-like behaviour, Nature 395 (1998) 686–689.
[39] P. Tackley, Self-consistent generation of tectonic plates in three-dimensional mantle convection, Earth Planet. Sci. Lett. 157 (1998) 9–22.
[40] D. Bercovici, Generation of plate tectonics from lithosphere-mantle flow and void-volatile self-lubrication, Earth Planet. Sci. Lett. 54 (1998) 139–151.
[41] J. Braun et al., A simple parameterization of strain localization in the ductile regime due to grain size reduction: A case study for olivine, J. Geophys. Res. 104 (1999) 25167–25181.
[42] M.C. Kameyama, D.A. Yuen, H. Fujimoto, The interaction of viscous heating with grain-size dependent rheology in the formation of localized slip zones, Geophys. Res. Lett. 24 (1997) 2523–2526.